

STRESS AND TEMPERATURE DEPENDENCE OF IRRADIATION CREEP OF SELECTED FCC AND BCC STEELS AT LOW SWELLING – M. B. Toloczko and F. A. Garner*

OBJECTIVE

The objective of this work was to show that a transition stress exists in FCC and BCC steels during irradiation creep and to map out this transition stress as a function of temperature and to propose possible creep deformation mechanisms taking place beyond the transition stress.

SUMMARY

A large amount of data on irradiation creep of face centered cubic (FCC) and body centered cubic (BCC) steels have been analyzed and published by the present authors, but a recent reanalysis of these data have provided further insight into irradiation creep behavior. The present paper looks at the stress and temperature dependence of creep at low swelling for selected 316 stainless steels and HT9 steels irradiated at temperatures from 400°C to 670°C. Analysis of the creep data has revealed that a transition from a lower creep rate with a stress exponent of one to a higher creep rate with an unknown stress exponent occurs in FCC and BCC steels at moderate stresses, and the transition stress is approximately the same for both classes of steels. Due to limited data at higher stresses, the nature of the creep behavior at stresses greater than the transition stress cannot be unambiguously defined. One possibility is that the stress exponent is transitioning from a value of one to a value greater than one. Another possibility is that the creep compliance value is transitioning to a higher value while the stress exponent remains at a value of one. The creep compliance coefficients of the FCC and BCC steels have also been carefully reanalyzed in the regime where the stresses are lower than the transition stress, and in this regime there is a clear delineation in the creep compliance values between 316 stainless steels, titanium-modified 316 steels, and HT9 steels as a function of temperature.

Introduction

In the present study, experimental data are reported which provide information on the irradiation creep phenomenon. It is understood that creep in an irradiation environment can be driven by a variety of mechanisms, and that like thermal creep, transitions in creep behavior may be observed in creep data as a function of applied stress. The present study uses a large body of creep data from a multi-year irradiation creep experiment that was performed in the Fast Flux Test Facility (FFTF) to define a temperature dependent transition stress. For stresses below this transition stress, there were sufficient data to determine the creep stress exponent and the creep compliance value, B_0 , but there was insufficient data to define either the creep stress exponent or the creep compliance for stresses greater than the transition stress. It was observed that the transition stress was approximately the same for 316 SS, titanium-modified 316 SS, and HT9 steel. From the examination of the creep compliance values at stresses below the transition stress, it will be concluded that the creep compliance is sensitive to composition and perhaps crystal system. Much of the creep data analyzed in the present study have been previously reported in the open literature [1-3], but the data have not been compiled and analyzed to show the stress and temperature dependencies to be reported.

Experimental

Materials and Specimens

The materials for this study were 316 stainless steel (SS), titanium-modified 316 SS, and HT-9 which is a ferritic-martensitic stainless steel. The composition and the pre-irradiation thermomechanical treatment of the FCC steels are shown in Tables 1 and 2, respectively, while the composition and pre-irradiation

* Pacific Northwest National Laboratory (PNNL) is operated for the U.S. Department of Energy by Battelle Memorial Institute under contract DE-AC06-76RLO-1830.

thermomechanical treatment for the BCC steels are shown in Tables 3 and 4, respectively. Fabrication of the pressurized tubes from tube-stock is described in [4].

For each target irradiation temperature, a set of capped thin-walled tubes were fabricated with each tube having a different pressure. For the present work, a set of pressurized tubes shall be called a tube-set. The range of pressures, and thus stresses, was chosen based on the target irradiation temperature. In general, a tube-set consisted of between four and eight pressurized tubes with one tube have zero pressure at the irradiation temperature. The zero stress tube was used to estimate swelling.

The uncertainty in the magnitude of the stress in the tube-wall arises mainly from deviations in the actual test temperature (T_{test}) from the target test temperature (T_{target}). First order error analysis shows that the uncertainty in the stress is given approximately by

$$\frac{\Delta\sigma}{\sigma} \sim \frac{|T_{\text{test}} - T_{\text{target}}|}{T_{\text{target}}} \quad (1)$$

where the temperature is in Kelvin.

Stress and Strain Calculations

The stress state in the wall of a capped thin-wall pressurized tube is well known [4,5], and shall not be repeated here. The stress state is biaxial, and for purposes of comparison to other specimen geometries and stress states, the creep data are examined as a function of the von Mises effective stress ($\bar{\sigma}$, which for pressurized tubes is given by

$$\bar{\sigma} = \frac{\sqrt{3}}{2} \sigma_H \quad (2)$$

where σ_H is the hoop (tangential) stress.

Due to the 2:1 ratio of the hoop stress to the axial stress, and due to the fact that creep involves only deviatoric deformation, a plane strain deformation condition exists when a pressurized tube undergoes creep. The deviatoric deformation lies in the $r\theta$ plane, and there is no deviatoric deformation along the z -axis. Creep strains are obtained from the change in the outer-wall diameter of a tube. This measured outer-wall strain is converted into a mid-wall strain which is an average of the strain across the tube-wall thickness. For the tube geometries utilized in this experiment, the conversion factor is of the order of 1.1 and is essentially constant for outer-wall strains up to 10%. The mid-wall strain (ϵ_M) is then converted to an effective plastic strain [6]. Assuming plane strain deformation in the $r\theta$ plane, the effective plastic

Table 1. Composition of the FCC steels for the present study.

Alloy	Fe	Cr	Ni	Mo	Mn	V	Al	Cu	Co
Ti-Mod 316SS†	Bal	13.7	15.8	1.65	2.03	0.01	<0.01	<0.01	<0.01
316SS 1 st Core	Bal	17.4	13.7	2.34	1.77	0.02	0.005	0.01	0.005
316SS 4 th Core	Bal	17.7	13.7	2.82	1.53	0.01	0.01	0.02	0.01
Alloy	Si	C	Ti	Ta	S	P	B	N	O
Ti-Mod 316SS	0.80	0.039	0.34	<0.01	0.003	0.005	0.0005	0.004	---
316SS 1 st Core	0.57	0.047	---	0.015	0.006	0.004	0.0005	0.004	0.002
316SS 4 th Core	0.54	0.056	---	0.01	0.005	0.002	0.0005	0.002	0.002

† Ti-Mod 316 SS: D9 Heat 83508, 1st Core 316 SS: Heat 81600, 4th Core 316 SS: Heat 93591

Table 2. Pre-irradiation thermomechanical treatment of the FCC steels.

Alloy and Heat	Thermomechanical Treatment	Tube Dimensions (cm)	
D9 Reference (Ti-Mod 316 SS)	20% cold-worked	0.584	outside diameter
		0.038	wall thickness
		2.82	length
D9-FV1 (Ti-Mod 316 SS)	10% cold-worked	0.457	outside diameter
		0.020	wall thickness
		2.24	length
D9-FV2 (Ti-Mod 316 SS)	20% cold-worked	0.457	outside diameter
		0.020	wall thickness
		2.24	length
316 SS 1 st Core and 316 SS 4 th Core	20% cold-worked	0.457	outside diameter
		0.020	wall thickness
		2.24	length

strain is given by

$$\bar{\epsilon} = \frac{2}{\sqrt{3}} \epsilon_M \quad (3)$$

Because of the plane strain deformation and the conservation of volume which occurs during creep of a pressurized tube capsule, the pressure and wall thickness both decrease in such a way that the stresses in the tube wall remain nearly constant for strains as large as 10%.

Swelling was monitored by measuring the diametral strain of the stress-free tube that was included in each tube-set. As it is known that swelling is enhanced in materials under an applied stress [2, 7-11], the swelling estimates from the stress-free tubes were a lower bound estimate of the swelling that occurred in the pressurized tubes. For selected 316 SS pressurized tubes where stress-enhanced swelling was suspected to be large, these tubes were sacrificed at the conclusion of the irradiation experiment, and density measurements were performed to obtain swelling in the pressurized tubes [2]. The stress-enhanced swelling data were used in conjunction with the stress-free swelling values to obtain estimates of the true swelling rate in the pressurized tubes where stress-enhanced swelling was thought to be large.

Irradiation Conditions

Irradiations were performed at the Fast Flux Test Facility located in Richland, Washington using the Materials Open Test Assembly [12,13]. Target irradiation temperatures ranged from 400°C to 670°C. Specimen irradiation temperatures were achieved using an actively controlled gas-gap method which permitted temperature control to within $\pm 5^\circ\text{C}$ [13]. In most every instance, pressurized tubes in a tube-set

Table 3. Composition of the BCC steels.

Alloy	Fe	Cr	Ni	Mo	Mn	V	W
HT9-1†	Bal	11.8	0.51	1.03	0.50	0.33	0.52
HT9-2,3	Bal	11.8	0.57	0.94	0.54	0.24	0.52
HT9-5	Bal	11.8	0.60	1.06	0.62	0.33	0.52
Alloy	Si	C	Ti	Al	S	P	N
HT9-1	0.21	0.21	< 0.01	0.03	0.003	0.008	0.006
HT9-2,3	0.28	0.17	< 0.01	0.05	0.003	0.007	0.006
HT9-5	0.29	0.21	---	0.01	0.002	0.011	---

† HT9-1: Heat 84425; HT9-2,3: Heat 91353; HT9-5: Heat 92235

Table 4. Pre-irradiation thermomechanical treatment of the BCC steels.

Alloy	Thermomechanical Treatment	Tube Dimensions (cm)
HT9-1 and HT9-2	1038°C/5 min/air cool, 760°C/30 min/air cool	0.457 outside diameter 0.020 wall thickness 2.24 length
HT9-3	1100°C/2 min/air cool, 650°C/2 hr/air cool	0.457 outside diameter 0.020 wall thickness 2.24 length
HT9-5	1100°C/2 min/air cool, 650°C/2 hr/air cool	0.686 outside diameter 0.055 wall thickness 2.82 length

were placed side-by-side in the reactor to provide nearly identical irradiation conditions within a tube-set. However, a tube-set was not necessarily kept in the same position from one irradiation cycle to the next, which occasionally resulted in small temperature differences from one irradiation cycle to the next. Depending on the location in reactor and the particular MOT cycle, the dose rate for this experiment ranged from $\sim 0.8 \times 10^{-6}$ dpa/sec to $\sim 1.7 \times 10^{-6}$ dpa/sec. Tubes were removed from reactor after each irradiation cycle, and diameter measurements were performed using a scanning laser profilometer [13]. Total accumulated dose ranged from about 50 dpa up to 165 dpa.

Creep Compliance Calculations

The creep compliance, B_0 , is defined by the equation

$$\frac{\dot{\epsilon}}{\bar{\sigma}} = B_0 + D\dot{S} \quad (4)$$

where $\dot{\epsilon}$ is the effective strain rate per dpa, D is the creep-swelling coupling coefficient, and \dot{S} is the volumetric swelling rate per dpa. B_0 represents the contribution to irradiation creep that is independent of swelling. For the present study, B_0 was calculated from the strains accumulated after the first irradiation cycle. For the HT9 and the Ti-modified 316 SS, no swelling was observed in the first irradiation cycle, and B_0 was easily calculated from Equation 4. However, for the 316 SS at several of the irradiation temperatures, swelling was observed during the first irradiation cycle. When swelling was present, it was necessary to solve for both B_0 and D which was done by applying Equation 4 to two irradiation intervals which provided the two equations needed to solve for the two unknowns, B_0 and D .

Results

Stress-Enhanced Swelling Measurements

316 SS is known to swell significantly at irradiation temperatures ranging from 550°C to 600°C, and thus it was necessary to measure both the stress-free swelling and the stress-enhancement of swelling so that the creep compliance could be accurately measured. Stress-enhanced swelling was measured on the 1st Core of 316 SS pressurized tubes irradiated at 550°C to about 80 dpa as previously reported [2]. The swelling in the pressurized tubes after 80 dpa along with the interpolated effect of stress on the swelling at lower doses is shown in Figure 1. The interpolated values for the swelling are represented by the equation

$$S = S_0(1 + F\bar{\sigma}) \quad (5)$$

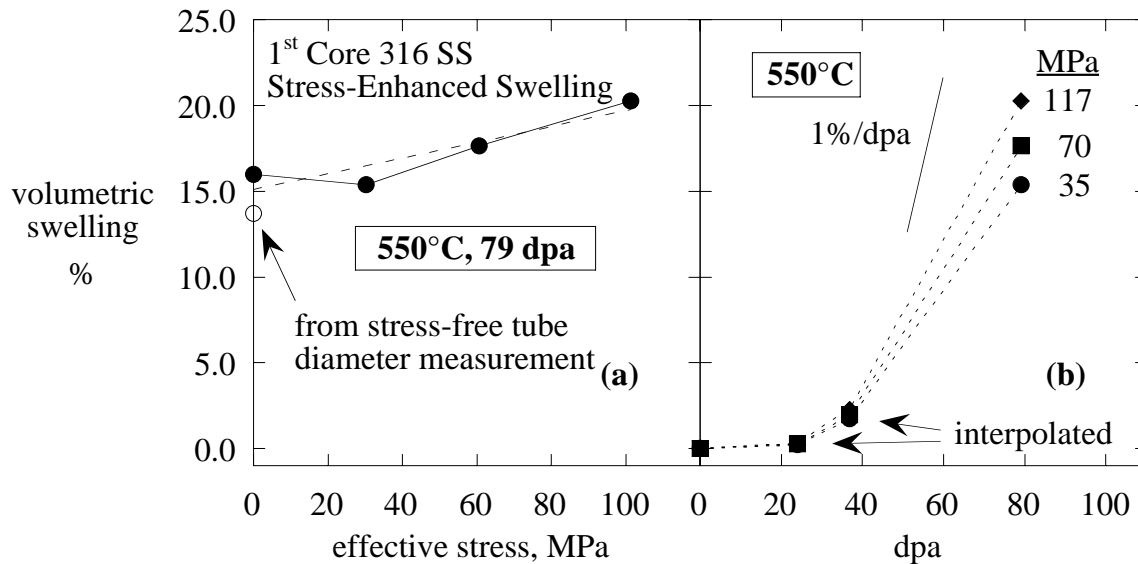


Figure 1. a) Stress-enhanced swelling of the 1st Core heat of 316 SS irradiated at 550°C, and b) the estimated interpolated behavior of the stress-enhanced swelling of the pressurized tubes at the lower doses.

where S_0 is the stress-free swelling, and F is a linear correlation factor. For the 316 SS, F was found to be $0.3 \times 10^{-2} \text{ MPa}^{-1}$ by fitting Equation 5 to the data in Figure 1a. As F will be used at temperatures other than at 550°C and only data on stress-enhanced swelling had been gathered at 550°C, the creep data in the open literature were surveyed to determine values for F at other temperatures. Creep data where F could be calculated were found for 316 SS and stabilized 316 SS irradiated at temperatures ranging from 455°C to 480°C, and the resulting F values are shown in Table 5. For swelling values greater than 1% where F could be clearly measured, F ranged from 0.3 - $0.9 \times 10^{-2} \text{ MPa}^{-1}$. It was decided to use a value for F of $0.5 \times 10^{-2} \text{ MPa}^{-1}$ which represents an average value over a greater range of temperatures.

Creep Data and Transition Stress

A vast amount of creep data were analyzed for the present study making it impractical to present all the creep data here, but a few representative plots showing creep strain as a function of applied stress are shown in Figures 2 and 3. The entire creep data set is published in Reference 14, and parts are published in References 1-3. The transition stress was taken at the data point on the creep versus stress curves where a large increase in slope occurred. Because there were only a limited number of data points on each curve, the chosen transition stress is a lower-bound estimate of the actual transition stress, and the actual transition stress may lie at some stress bounded by the chosen transition stress and the next higher stress level. Figure 3 shows an example where a transition in creep rate as a function of stress is clearly apparent. It was observed that the transition stress was temperature dependent, and the transition stress is plotted as a function of temperature in Figure 4. The data points connected by the dotted lines represent the maximum applied stress at that temperature, while the data points connected by the solid lines represent the transition stress. There were two instances where the maximum applied stress may not have been high enough to reach the transition stress. The first is at 400°C where it can be seen that the maximum applied stress is 173 MPa, and all three of the alloy types showed no transition behavior up to this stress level. The other instance is at 600°C where the maximum applied stress of the HT9 alloy was only 15 MPa. Again, no transition in creep behavior was observed up to this stress, and the actual transition stress may have been greater than 15 MPa.

Table 5. Values for the stress-enhanced swelling coefficient calculated from data published in the open literature.

$S = S_0(1 + F\bar{\sigma})$			
reference	irradiation conditions	S_0 , %	F , $\times 10^{-2} \text{ MPa}^{-1}$
7	annealed 316SS PT, 500°C	0.035	2.6
8	20% CW 316SS PT, 477°C	1.6	0.38
9	CW 316SS + Nb PT, 480°C	3.3	0.63
10	CW 316SS + Ti PT, 455°C	4.0	0.89
11	SA 316 type + Nb Pt, 480°C	20	0.30

Stress and Temperature Dependence of the Creep Stress Exponent

From plots of creep strain as a function of stress it was possible to determine the stress exponent for irradiation creep for stresses below the transition stress. For stresses above the transition stress, there were insufficient data to determine the creep stress exponent (or the creep compliance). For this study, creep strain as a function of stress was examined for the three alloy types at temperatures ranging from 400°C to 670°C which permits determining the stress exponent as a function of both stress and temperature. For stresses up to the transition stress, it was observed that the creep stress exponent had a value of one for each of the different alloy types.

Temperature Dependence of the Creep Compliance

The creep compliance coefficient of the alloys within the regime of stresses and temperatures where the stress exponent is equal to one is shown as a function of irradiation temperature in Figure 5a. As can be seen, there are clear differences in the creep compliance values for the three alloys with HT9 having the lowest creep compliance coefficient for temperatures between 400°C and 600°C. Shown in Figure 5b are creep compliance coefficient values obtained from creep data in the literature on similar materials [9, 15-26]. The values for the creep coefficients for the alloys in the literature are not so well stratified, but one similar trend is that with the exception of Malliard's data [22] which are unreasonably low for those

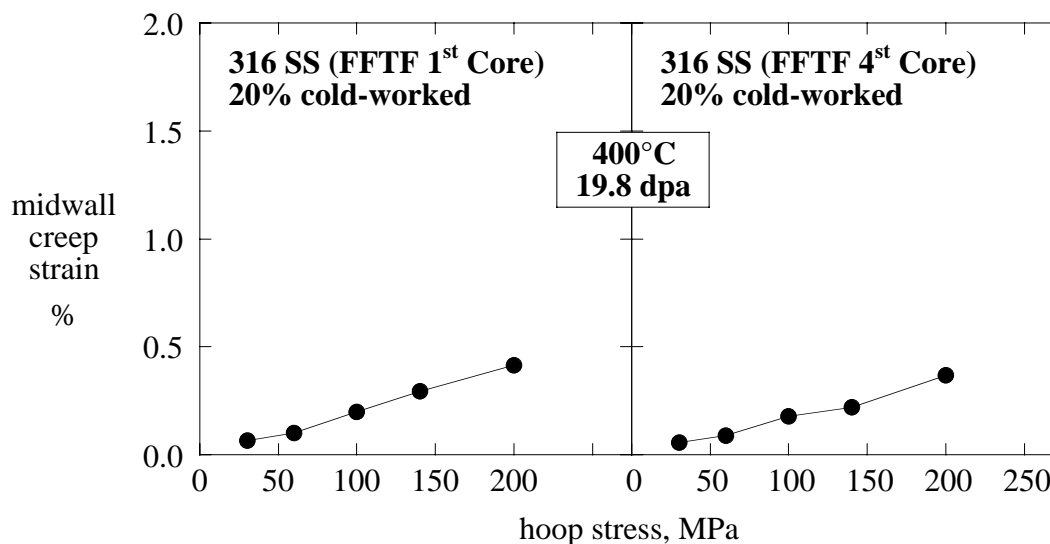


Figure 2. Midwall creep strain as a function of stress for two heats of 316 SS irradiated at 400°C.

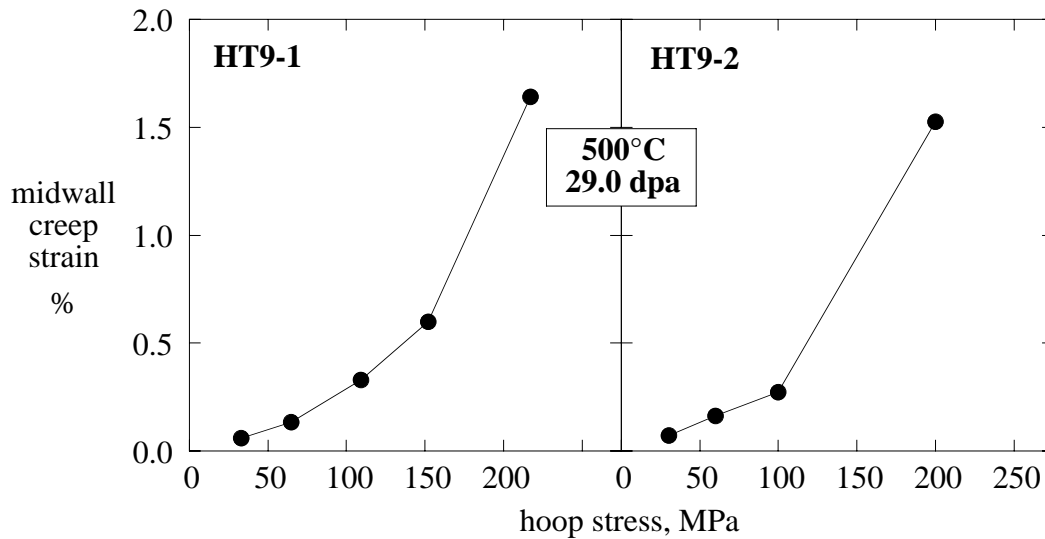


Figure 3. Midwall creep strain as a function of stress for two heats of HT9 irradiated at 500°C.

temperatures, the Ti-mod 316 SS alloys consistently have the highest creep compliance coefficient at the lower temperatures as does the Ti-mod 316 SS variants in the present study. The creep compliance values for the HT9 and 316 SS in the literature appear to be approximately the same.

Discussion

Transition Stress and Creep Mechanisms

A transition stress is typically representative of a change in creep mechanism. For the present study, a stress exponent of one at stresses below the transition stress indicates that a mechanism based on point defect diffusion is dominating irradiation creep. In the regime of temperatures where irradiation creep is known to be dominant (below 550°C in steels), current theories suggest that dislocation climb driven by point defect diffusion is the primary creep mechanism [27-30]. Because of the limited amount of data at stresses above the transition stress, it was not possible to determine whether the increase in creep as a function of stress was indicative of an increase in stress exponent or simply an increase in the creep compliance.

As a way to attempt to rationalize the creep mechanisms above and below the transition stress, the transition stress line for the irradiated 316 SS was overlaid on a thermal creep deformation map of 316 SS taken from the literature [31]. Ideally, the thermal creep deformation map would have been for a 316 SS with the same microstructural features that are typically present in 316 SS after irradiation, but such materials and deformation maps are not available. Instead, the thermal creep deformation map was for annealed 316 SS. The thermal creep deformation map with the transition stress for the irradiated 316 SS is shown in Figure 6. This is not an ideal comparison because there are many differences in the microstructures of the two materials being compared. The annealed material will have a low dislocation density of about 10^8 cm^{-2} , it is free of precipitates, and it has a grain size of about 50 μm , whereas the irradiated material is likely to have a temperature dependent dislocation density ranging from 10^{11} cm^{-2} at 400°C to about 10^8 cm^{-2} at 670°C, it will have a large number of precipitates (also temperature dependent), and it will have a grain size closer to 15 μm . Because of the differences in microstructure, if the irradiated material was placed under stress in a thermal environment and a creep deformation map were constructed, the boundary between elastic behavior and power-law creep for this material would likely be shifted to higher stresses relative to the annealed material, and the diffusional flow regime (as

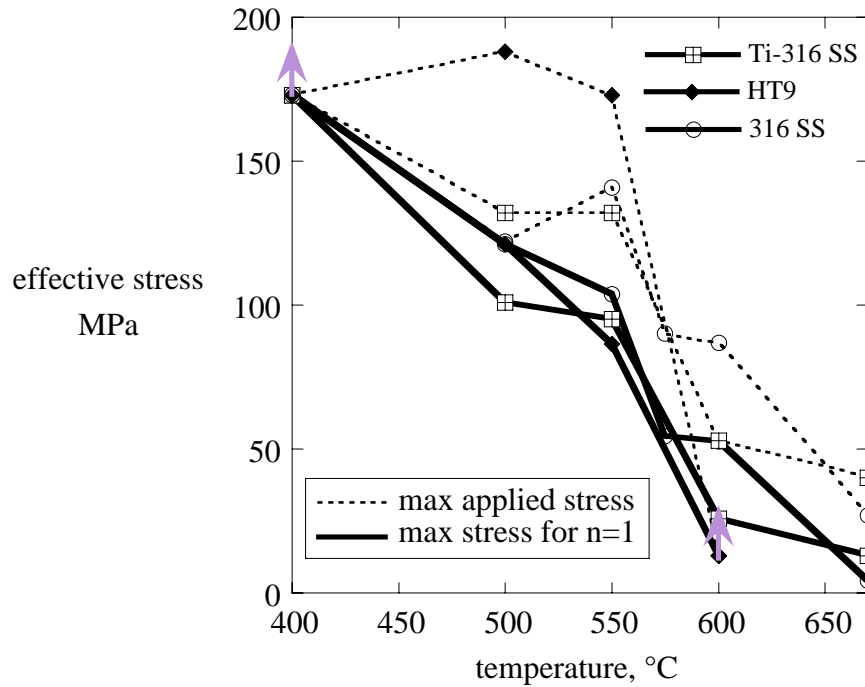


Figure 4. Transition stress as a function of temperature for the three alloy types. The data points associated with the solid lines represent the highest stress at which the creep rate was linearly proportional to the applied stress at the given temperature. The data points associated with the dotted lines represent the highest applied stress at the given temperature. The arrows indicate the transition stress was probably higher than the value shown because the maximum applied stress was not great enough to reach the transition stress.

defined in Figure 6) would be likely to have contributions by climb of dislocations at the lower temperatures. With this in mind, it is useful to compare the transition stress to the thermal creep behavior of the annealed material. Between 400°C and 550°C, the transition stress straddles the boundary between elastic behavior and power-law creep suggesting that at these temperatures, an irradiation-assisted climb-glide creep mechanism [31-35] may be beginning to play a dominant role in the total creep strains at stresses beyond the transition stress. This would lead to an increase in the creep stress exponent at stresses beyond the transition stress. At temperatures between 550°C and 670°C, it appears that diffusionally-controlled thermal creep mechanisms may be beginning to play a role in the total creep strains. In this scenario, thermal creep is likely to be driven by Coble creep mechanisms, and the creep stress exponent above the transition stress would remain at a value of one. While this discussion was based on trends in 316 SS, it is likely that similar phenomenon are occurring in the Ti-modified 316 SS and the HT9 variants.

Temperature Dependence of the Creep Compliance

The creep compliance values in Figure 5a show some unexpected trends. Because BCC steels are generally believed to have lower thermal creep resistance than FCC steels at high temperatures, it has been assumed that BCC steels would have lower creep resistance than FCC steels when irradiated at temperatures of 600°C and beyond. The data in Figure 5a, however, suggest that BCC steels may actually perform better in an elevated temperature irradiation environment than FCC steels. As discussed, it is likely that at temperatures of 550°C and beyond, thermal creep is likely to be playing a more and more dominant role. So it seems possible that the large increase in the creep compliance values for the 316 SS variants is due to thermal creep mechanisms, and it may be that for the relatively

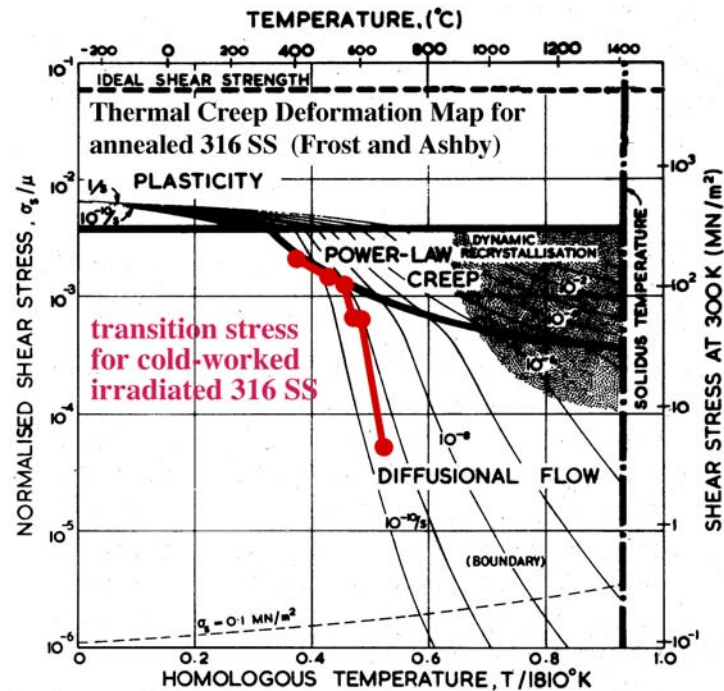


Figure 6. Creep deformation map of annealed 316 SS overlaid with the transition stress for 20% cold-worked irradiated 316 SS.

microstructure of BCC steels is more resistant to irradiation-induced microstructure changes than FCC steels.

REFERENCES

- [1] F. A. Garner, M. L. Hamilton, C. R. Eiholzer, M. B. Toloczko, and A. S. Kumar, "Irradiation and thermal creep of a titanium-modified austenitic stainless steel and its dependence on cold work level", *Journal of Nuclear Materials*, Vols. 191-194, 1992, pp. 813-817.
- [2] F. A. Garner, M. B. Toloczko, and R. J. Puigh, "The Relationship Between Swelling and Irradiation Creep in 20% Cold-Worked 316 Stainless Steel", *Effects of Radiation on Materials*, 19th International Symposium, ASTM STP 1366, M. L. Hamilton, A. S. Kumar, S. T. Rosinski, and M. L. Grossbeck, Eds., American Society for Testing and Materials, West Conshohocken, PA, 1999, pp. 667-678.
- [3] M. B. Toloczko, and F. A. Garner, "Variability of Irradiation Creep and Swelling of HT9 Irradiated to High Neutron Fluences at 400-600°C", *Effects of Radiation on Materials: 18th International Symposium*, ASTM STP 1325, R. K. Nanstad, M. L. Hamilton, F. A. Garner, and A. S. Kumar, Eds., American Society for Testing and Materials, West Conshohocken, PA, 1999, pp. 765-779.
- [4] M. B. Toloczko, B. R. Grambau, F. A. Garner, and K. Abe, "Comparison of Thermal Creep and Irradiation Creep of HT9 Pressurized Tubes at Test Temperatures From ~490°C to 605°C", *Effects of Radiation on Materials: 20th International Symposium*, ASTM STP 1405, S. T. Rosinski, M. L. Grossbeck, T. R. Allen, and A. S. Kumar, Eds., American Society for Testing and Materials, West Conshohocken, PA, 2001, pp. 557-569.

- [5] S. P. Timoshenko, J. N. and Goodier, *Theory of Elasticity, Third Edition*, McGraw-Hill Book Company, 1970.
- [6] L. E. Malvern, *Introduction to Mechanics of a Continuous Medium*, Prentice-Hall, Inc., New Jersey, 1969.
- [7] J. F. Bates and E. R. Gilbert, "Experimental Evidence for Stress Enhanced Swelling", *Journal of Nuclear Materials*, Vol. 59, 1976, p. 95.
- [8] J. F. Bates and E. R. Gilbert, "Effects of Stress on Swelling in 316 Stainless Steel", *Journal of Nuclear Materials*, Vol. 71, 1978, p. 286.
- [9] W. Schneider, K. Herschbach, and K. Ehrlich, "Interdependence of In-Pile Creep and Void Swelling in Ti- and Nb-Stabilized Stainless Steels", *ASTM STP 782*, 1982, p. 30.
- [10] J. L. Seran, H. Touron, A. Maillard, P. Dubuisson, J.P. Hugot, E. Le Boulbin, P. Blanchard, and M. Pelletier, "The Swelling Behavior of Titanium-Stabilized Austenitic Steels Used as Structural Materials of Fissile Subassemblies in Phénix", *ASTM STP 1046*, 1990, p. 739.
- [11] A. N. Vorobjev, N. I. Budykin, E. G. Mironova, S. I. Porollo, Yu. V. Konobeev, and F. A. Garner, "Irradiation Creep and Stress-Enhanced Swelling of Fe-16Cr-15Ni-Nb Austenitic Stainless Steel in BN-350", *Journal of Nuclear Materials*, Vols. 258-263, 1998, p. 1618.
- [12] Irradiation Parameters for the FFTF Materials Open Test Assemblies from 1983 to 1992, WHC-SD-FF-TD-010 Revision 0, August, 1994.
- [13] E. R. Gilbert, and B. A. Chin, "Irradiated Materials Measurement Technology," *Effects of Radiation on Materials: Tenth Conference, ASTM STP 725*, David Kramer, H. R. Brager, J. S. Perrin, Eds., American Society for Testing and Materials, Philadelphia, 1981, pp. 665-679.
- [14] M. B. Toloczko, "Irradiation Creep of Stainless Steels", Ph.D. Thesis, Washington State University, Pullman, WA, December, 1999.
- [15] E. R. Gilbert and J. F. Bates, "Dependence of Irradiation Creep on Temperature and Atom Displacements in 20% Cold-Worked Type 316 Stainless Steel", *Journal of Nuclear Materials*, Vol. 65, 1977, p. 204.
- [16] J. L. Boutard, Y. Carteret, R. Cauvin, Y. Guerin, and A. Maillard, "Irradiation Creep of Solution Annealed and Cold-Worked 316 Stainless Steel", *Proceedings of the Conference on Dimensional Stability and Mechanical Behaviour of Irradiated Metals and Alloys*, Vol. 1, British Nuclear Energy Society, 1983.
- [17] G. W. Lewthwaite and D. Mosedale, "The Creep of Solution Annealed, Austenitic Stainless Steels at about 500 K in the Dounreay Fast Reactor, (DFR)", *Proceedings of the Conference on Dimensional Stability and Mechanical Behaviour of Irradiated Metals and Alloys*, Vol. 1, British Nuclear Energy Society, 1983.
- [18] K. Herschbach, W. Schneider, and H. J. Bergmann, "Swelling and In-Pile Creep Behavior of Some 15Cr15TiNi Stainless Steels in the Temperature Range 400 to 600°C", *ASTM STP 1046*, 1990, p. 570.
- [19] D. L. Porter, G. D. Hudman, F. A. Garner, "Irradiation Creep and Swelling of Annealed Type 304L Stainless Steel at ~390°C and High Neutron Fluence", *Journal of Nuclear Materials*, Vols. 179-181, 1991, p. 581.

- [20] J. L. Séran, V. Lévy, P. Dubuisson, D. Gilbon, A. Maillard, A. Fissolo, H. Touron, R. Cauvin, A. Chalony, and E. Le Boulbin, "Behavior under Neutron Irradiation of the 15-15Ti and EM10 Steels Used as Standard Materials of the Phénix Fuel Subassembly", ASTM STP 1125, 1992, pg. 1209.
- [21] V. S. Neustroev and V. K. Shamardin, "Radiation Creep and Swelling of Austenitic 16Cr-15Ni-3Mo-Nb Steels Irradiated in the Reactor BOR-60 at 350 and 420 C", ASTM STP 1175, 1993, p. 816.
- [22] A. Maillard, H. Touron, J. L. Séran, and A. Chalony, "Swelling and Irradiation Creep of Neutron-Irradiated 316Ti and 15-15Ti Steels", ASTM STP 1175, 1994, p. 824.
- [23] M. L. Grossbeck, L. T. Gibson, and S. Jitsukawa, "Irradiation Creep in Austenitic and Ferritic Steels Irradiated in a Tailored Neutron Spectrum to Induce Fusion Reactor Levels of Helium", Journal of Nuclear Materials, Vols. 233-237, 1996, p. 148.
- [24] I. Shibahara, S. Ukai, S. Onose, and S. Shikakura, "Irradiation Performance of Modified 316 Stainless Steel for Monju Fuel", Journal of Nuclear Materials, Vol. 204, 1993, p. 131.
- [25] B. A. Chin, "An Analysis of the Creep Properties of a 12Cr-1Mo-W-V Steel", Proceedings of: Topical Conference on Ferritic Alloys for the use in Nuclear Energy Technologies, Snowbird, UT, 1983, p. 593.
- [26] R. J. Puigh, "In-Reactor Creep of Selected Ferritic Alloys", ASTM STP 870, 1985, p. 7.
- [27] P. T. Heald and M. V. Speight, "Steady-State Irradiation Creep", Philosophical Magazine, Vol. 29, 1974, p. 1075.
- [28] W. G. Wolfer and M. Ashkin, "Diffusion of Vacancies and Interstitials to Edge Dislocations", Journal of Applied Physics, Vol. 47, No. 3, 1976, p. 791.
- [29] F. R. N. Nabarro, R. Bullough, and J. R. Matthews, "The Enhancement of Creep by Irradiation", Acta Metallurgica, Vol. 30, 1982, p. 1761.
- [30] C. H. Woo, "Shape Effect in the Drift Diffusion of Point Defects into Straight Dislocations", Physical Review B, Vol. 30, No. 6, 1984, p. 3084.
- [31] H. J. Frost and M. F. Ashby, "Deformation-Mechanism Maps, The Plasticity and Creep of Metals and Ceramics" 1st Edition, Pergamon Press Inc, 1982.
- [32] J. Weertman, "Dislocation Climb Theory of Steady State Creep", Transactions of the American Society for Metals, Vol. 61, 1968, p. 681.
- [33] S. D. Harkness, J. A. Tesk, and C.-Y. Li, "An Analysis of Fast Neutron Effects on Void Formation and Creep in Metals", Nuclear Applications and Technology, Vol. 9, 1970, p. 24.
- [34] L. K. Mansur, "Irradiation Creep by Climb-Enabled Glide of Dislocations Resulting from Preferred Absorption of Point Defects", Philosophical Magazine A, Vol. 39, No. 4, 1979, p. 497.
- [35] J. H. Gittus, R. G. Anderson, and M. J. Makin, "On the Possibility that Cottrell Creep occurs when Non-Fissile Materials such as Stainless Steel Irradiated in a Fast Reactor", Proceedings of the conference on Irradiation Embrittlement and Creep in Fuel Cladding and Core Components, British Nuclear Energy Society, 1972, pg. 291.

- [36] W. J. Duffin and F. A. Nichols, "The Effect of irradiation on Diffusion-Controlled Creep Processes", *Journal of Nuclear Materials*, Vol. 45, 1972/73, p. 302.
- [37] F. Garofalo, "Fundamentals of Creep and Creep-Rupture in Metals", The MacMillian Company, New York, 1965.
- [38] J. P. Hirth and J. Lothe, "Theory of Dislocations", 2nd Edition, Wiley and Sons, Inc., 1982.